Applied Physics Letters

RESEARCH ARTICLE | SEPTEMBER 05 2023

# Low fluorescence crosstalk patterning of quantum dots based on laser drilling and micropore filling

Jiwei Li ; Kaifeng Zheng; Wenchao Sun ; Licai Zhu; Jin Tao ; Panyuan Li; Kaili Fan ; Jinguang Lv; Yuxin Qin; Baixuan Zhao; Yingze Zhao; Yupeng Chen; Jingqiu Liang ; Weibiao Wang



*Appl. Phys. Lett.* 123, 101101 (2023)
https://doi.org/10.1063/5.0161855

Applied Physics Letters ARTICLE pubs.aip.org/aip/apl

# Low fluorescence crosstalk patterning of quantum dots based on laser drilling and micropore filling

Cite as: Appl. Phys. Lett. **123**, 101101 (2023); doi: 10.1063/5.0161855
Submitted: 12 June 2023 · Accepted: 19 August 2023 ·
Published Online: 5 September 2023



Jiwei Li,[1,2] Kaifeng Zheng,[1] Wenchao Sun,[1,2] Licai Zhu,[1,2] Jin Tao,[1] Panyuan Li,[1,2] Kaili Fan,[1,2] Jinguang Lv,[1] Yuxin Qin,[1] Baixuan Zhao,[1] Yingze Zhao,[1] Yupeng Chen,[1] Jingqiu Liang,[1,a)] and Weibiao Wang[1,a)]

## AFFILIATIONS

[1]State Key Laboratory of Applied Optics, Changchun Institute of Optics, Fine Mechanics and Physics, Chinese Academy of Sciences, Changchun, Jilin 130033, China

[2]University of Chinese Academy of Sciences, Beijing 100049, China

[a)]Authors to whom correspondence should be addressed: liangjq@ciomp.ac.cn and wangwb@ciomp.ac.cn

## ABSTRACT

In this study, a dual-color patterned perovskite quantum dot color conversion layer with a light-blocking matrix was created by combining laser drilling with micropore filling technology. When the blue micro-LED and the quantum dot color conversion layer make contact, the fluorescence crosstalk effect can be simulated to be near zero. The color conversion layers with high color gamut (111.2% of the National Television System Commission) were further confirmed to have outstanding optical isolation performance through experimental observations. This work may have significant advantages for its applications in photonic integration, micro-LED, and near-field displays due to simple operation process, maskless, harmlessness to quantum dots, short process period, and low crosstalk effect.





Micro-LED is widely considered as the next-generation display technology following liquid crystal and organic light emitting devices (LCD and OLED) owing to its high resolution and contrast, quick response time, low energy consumption, and prolonged lifetime.[1–3] Full-color display technology of micro-LED is critical to its industrialization, which can be achieved mainly through massive transfer and quantum dot color conversion layers (QDCCLs).[4] Massive transfer technology involves attaching millions of different micro-display chips to the same target substrate, but it faces significant obstacles in commercialization, such as low production rate, high maintenance cost, and testing expense.[2,5] Quantum dots (QDs) featured solution processability, facile color tunability, narrow emission bandwidth, and high luminescence efficiency and can be excited by blue or ultraviolet micro-LED to emit red–green–blue light as color conversion layers.[6–8] Inkjet printing,[9–13] and lithography[14–16] are two traditional methods of patterning QDs. Inkjet printing is commonly utilized due to its benefits of non-contact processing, material efficacy, and repeatable processability, but it has also some drawbacks, such as poor edge morphology, QD aggregation, thin QD film layer, high cost, and operational complexity, which affect its application in display.[17–21] High pixel density can be achieved by the photolithography technique but results in significant QD waste and degradation of the photoluminescence properties of QDs when photoresist doped with QD is used.[22–25]

In the article, we propose a simple and low fluorescence crosstalk method for patterning full-color QDCCLs on a black SU8 photoresist mold (BM) utilizing micropore filling[26] and laser drilling technology.[27,28] Laser drilling is an advanced machining technology that employs a maskless and no lithography process, which significantly avoids pollution and damage to QDs. The high degree of automation, precision, and efficiency of laser drilling allow for QDCCL fabrication with short processing time, low cost, and high resolution. As a result, advantages of laser drilling combined with the straightforward operation of the micropore filling technique make it easier to manufacture the high-quality perovskite quantum dot color conversion layers (PQDCCLs). Additionally, systematic simulation and experimental observation revealed that the light crosstalk effect between adjacent pixels was significantly suppressed by using the black SU8 photoresist as a light-blocking matrix, as opposed to the transparent SU8 photoresist mold (TM). Based on this method, the single-color and dual-color PQDCCLs with a minimum micropore diameter of 35 $\mu$m were fabricated.

For the preparation of single-color QDCCLs, four key steps are involved in Fig. 1(a): laser drilling [the operating equipment is shown in Fig. S1(a)], PQD gel filling, UV exposure curing, and surface polishing. The BM (the detailed manufacturing technique is displayed in the supplementary material) was first made by laser drilling, and the

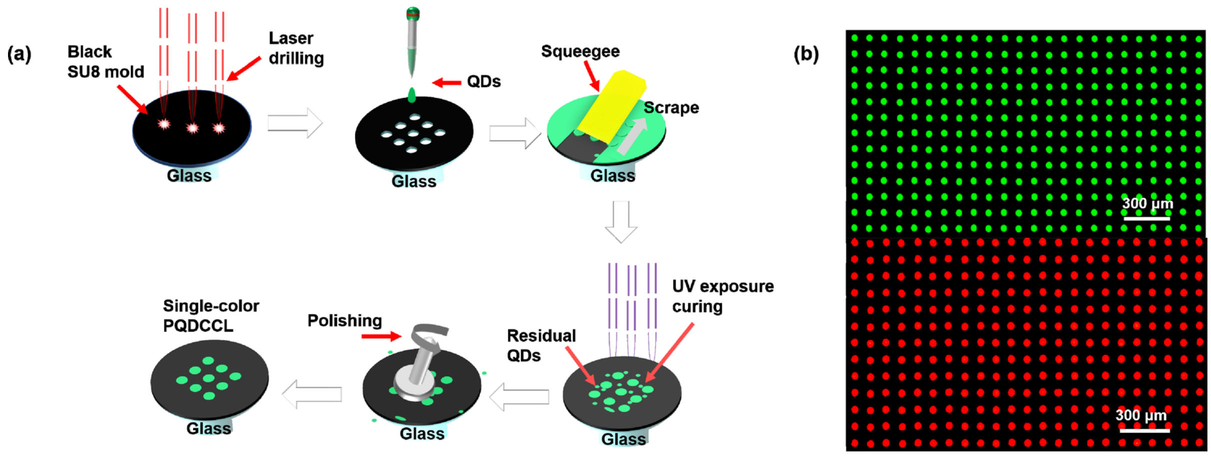


FIG. 1. (a) Preparation process of monochrome patterned QDCCLs by laser drilling and micropore filling technology. (b) Green and red PQDCCLs with pixel sizes of 100 $\mu$m and micropore diameter of 40 $\mu$m under a fluorescence microscope.

corresponding optical microscopy images are shown in Fig. S1(b). Following that, a dropper was used to drop the green or red PQD UV curing gel (the detailed fabrication technique of PQDs refers to supplementary material) on a BM. The surface of the micropore mold was then repeatedly scratched and coated with a squeegee so that the PQD gel could fill into the micropore. To facilitate the next production of dual-color PQDCCLs, the PQD gel must be exposed to ultraviolet light with lower power for 3 min after scraping. Finally, the fluorescent images of PQDCCLs shown in Fig. 1(b) were obtained after the residual PQDs were removed via the polishing process. The manufacturing process of the QDCCLs took place at room temperature, which ensured no harm to the PQDs.

We fabricated additional red and green PQD patterns [Figs. 2(a) and 2(b)] with the pixel sizes of 80 $\mu$m [Fig. 2(a)] and 60 $\mu$m [Fig. 2(b)] under a fluorescence microscope. The size of the single micropore, the distance between the adjacent micropores, and the depth of a single PQD pixel can be altered by adjusting the power, scanning space of the fiber laser, and thickness of the BM. By varying the power and scanning speed of the fiber laser, micropores with different diameters could be attained, e.g., as represented in Figs. 2(a) (50 $\mu$m for green



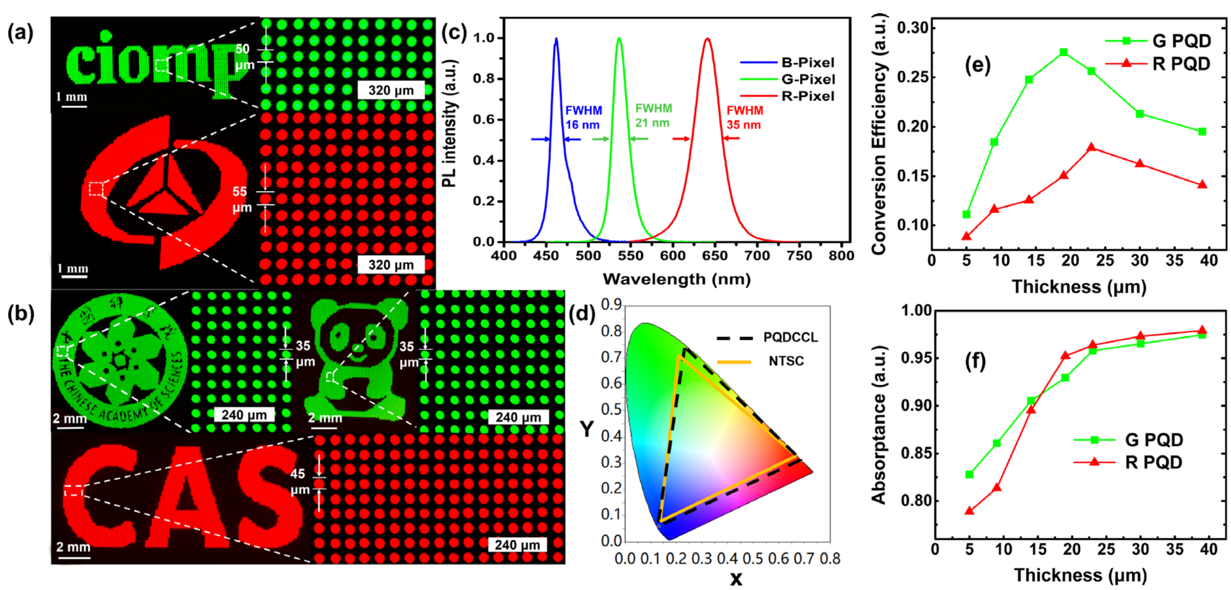


FIG. 2. Fluorescence images: (a) The English abbreviation (green letters "ciomp") and the emblem (red image) of our school and (b) the logo (the green image on the left) and English abbreviation (red letters "CAS") of Chinese Academy of Sciences and a vivid "panda" excited by 365 nm UV light. (c) Fluorescence spectra of green and red perovskite QDs microarrays excited by 465 nm blue light and spectra of exciting light from blue micro-LED. (d) The color gamut of PQDCCLs, when excited by blue micro-LED, and the color gamut of NTSC. (e) The color conversion efficiency and (f) absorptance curve of PQD Pixels at various thicknesses.

and 55 $\mu$m for red QD arrays) and 2(b) (35 $\mu$m for green and 45 $\mu$m for red QD arrays). Due to the limitation of fiber laser light spot, it is difficult for the micropore to achieve a very small diameter size below 35 $\mu$m via laser drilling. However, using femtosecond laser processing technology or designing an appropriate optical lens structure,[28–30] it will be simple to obtain micropores as small as several micrometers and even sub-microns, leading to an extension of applications to AR/VR displays. When excited by a blue micro-LED with a wavelength of 465 nm and a full-width at half-maximum (FWHM) of 16 nm, the red and green PQD arrays exhibit a narrow fluorescence emission peak maximum intensity at 536 and 641 nm respectively, with FWHM of 21 and 35 nm, as shown in Fig. 2(c). The color space of the PQDCCL coverage reaches 111.2% of the National Television System Commission (NTSC) standard, as depicted in Fig. 2(d). The thickness of BM with a range from 5 to 50 $\mu$m is closely related to the speed at which the photoresist is spun onto the glass substrate, which is equivalent to the thickness of a single PQD pixel. However, the self-absorption phenomena of QD pixels grows with thickness, leading to a decrease in color conversion efficiency. Figure 2(e) illustrates the color conversion efficiency of green and red PQDs under different thicknesses, with the maximum value of 27.551% for green PQD pixels at 19 $\mu$m and 17.873% for red PQD pixels at 23 $\mu$m, respectively. Therefore, the thickness of the QD film selected in this article is approximately about 20 $\mu$m. Figure 2(f) illustrates the absorbance curve of green and red PQDs as a function of the thickness, reaching 92.9% and 95.2% at the thickness of 19 and 23 $\mu$m for green and red PQDs, respectively.

The dual-color QDCCLs (the detailed preparation process is described in the supplementary material) were manufactured by reusing the micropore filling and laser drilling method, which are depicted in Fig. 3(a). The second graph depicted in Fig. 3(a) displays a PQDCCL that involves two sets of micropore arrays—one with PQDs and the other without PQDs, and the corresponding optical microscopy image is displayed in Fig. S2(a). To facilitate light emission from the blue micro-LED, a third set of micropore arrays without PQDs were created in the final step of Fig. 3(a) using the dual-color QDCCL as the mold, whose optical microscopy image is displayed in Fig. S2(b). Furthermore, the dual-color photo of a car with a pixel size of 100 $\mu$m is shown in Fig. 3(b), demonstrating the flexibility and

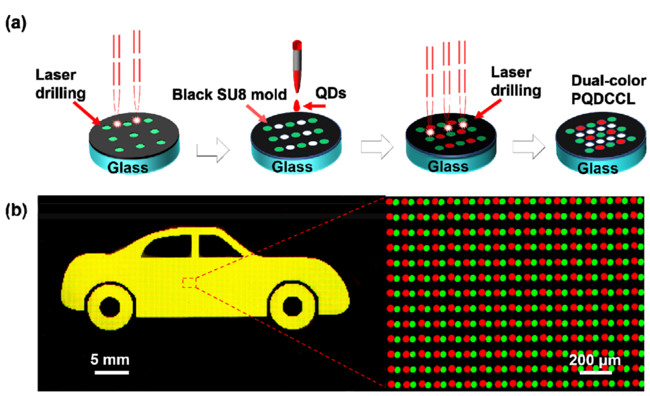


FIG. 3. (a) Fabrication process of dual-color QDCCLs. (b) A dual-color car image under a fluorescence microscope with a pixel size of 100 $\mu$m and its locally enlarged QD arrays.

feasibility of our QDCCL fabrication method, which further promote the development of full-color displays based on micro-LED.

Due to the wide view-angle feature of a single QD pixel, conventional patterned QDCCL structures without a light-blocking matrix are susceptible to severe light crosstalk effects among adjacent pixels. Therefore, to further investigate the factors related to the crosstalk effect in this study, a structure comprising a single blue micro-LED pixel and five QD pixels on the BM or TM was proposed, as shown in Figs. S3(a) and S3(b). Focused on this structure, the fluorescence crosstalk value was defined as[31]

$$\text{Fluorescence crosstalk ratio}\,(FCR)\%\,\frac{F_{\text{adj-pixel}}}{F_{\text{pixel}}} \times 100\%, \tag{1}$$

where "$F_{\text{pixel}}$" represents the fluorescence luminance of the QD pixel aligned to the blue micro-LED and "$F_{\text{adj-pixel}}$" represents the fluorescence luminance of the adjacent QD pixel. In this model, two components are considered to contribute to the fluorescence crosstalk effect: the gap, which is the vertical distance between the blue micro-LED and QDCCLs, and the space, which is the blank distance between adjacent QD sub-pixels, as shown in Fig. S3(a). Prior to simulating fluorescence crosstalk effects, the transmittance of SU8 photoresist film was measured at various thicknesses. Figure S4 shows that when the thickness of the black SU8 film exceeds 9 $\mu$m, the transmittance in the green and red spectral regions (with central wavelengths at 536 and 641 nm, respectively) is below 20%. However, when the thickness increases to more than 23 $\mu$m, the transmittance plummets to less than 3% and 1.3% for the red and green spectral regions, respectively. In contrast, the transparent SU8 film with a thickness of 25 $\mu$m has a transmittance higher than 95% across the entire light emission range from 500 to 800 nm.

To simplify the simulation process, only green PQDs were utilized in the model, where, in addition to the central QD sub-pixel, four other QD sub-pixels with different spaces (9, 15, 19, and 23 $\mu$m) from the central QD sub-pixel were constructed on the SU8 micropore mold with a radius of 100 $\mu$m, as depicted in Fig. S3(b). The final simulation results of FCR are shown in Fig. 4(a), which clearly illustrates severe fluorescence crosstalk in the TM, but none in the BM. Even when the gap is zero, FCR for the TM is still more than 5.9% in spite of the space. In contrast, FCR for the BM is nearly zero under the same conditions. As the gap increases to 14 $\mu$m and the space decreases to 9 $\mu$m, FCR for the TM increases to 12.3%, which is significantly higher than that (FCR = 3.45%) of the BM. In conclusion, the introduction of a BM is an efficient method of curbing fluorescence crosstalk in comparison to the utilization of a transparent one.

Figure 4(b) depicts the view-angle light intensity profile of single QD pixel with the size of 0.5 mm diameter on both the BM and TM by the experiment observation. The use of the BM significantly reduces the view angle at a half-brightness maximum from 58° to 25°, as marked by the red dashed line in Fig. 4(b), compared to the TM. The top views of the light beam profile emanating from a single-color PQD pixel on the BM or TM are illustrated in the insets on the upper right and lower right of Fig. 4(b), respectively. It is noteworthy that the light beam emission profile of single-color PQD pixel on the TM is more divergent than that on the BM, thus further demonstrating the remarkable light-blocking ability of the BM.

Ensuring homogeneity in light-emitting brightness is a critical factor in determining the display performance of QDCCLs. As shown

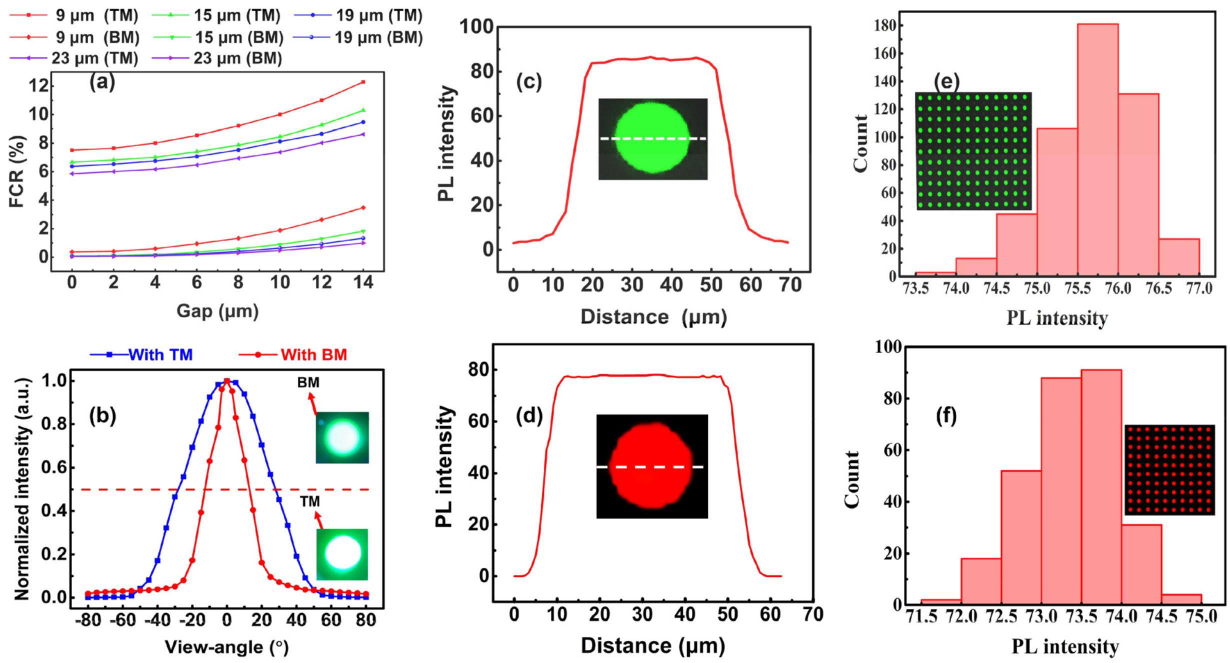


**FIG. 4.** (a) The crosstalk simulation result for PQDCCLs excited by blue micro-LED under different spaces. (b) The light intensity distribution curve of single perovskite QD pixel with the size of 0.5 mm diameter excited by 465 nm blue LED under different view angles by the experimental observation. (c) and (d) Radial fluorescence intensity distributions of a green and a red single micropore QD. (e) and (f) The corresponding average fluorescence intensity distribution statistical histograms of a green PQD array composed of 28 × 18 micropores with a diameter of 40 $\mu$m and a red PQD array composed of 23 × 13 micropores with a diameter of 45 $\mu$m under 365 nm UV light excitation.

in Figs. 4(c) and 4(d), the photoluminescence (PL) intensity distributions of the individual green and red QD pixels along the white dashed line in the inset indicate uniform PL intensity with minimal fluctuations along the diameter direction. Additionally, the local fluorescence graphs of a green PQD array composed of 28 × 18 micropores with a diameter of 40 $\mu$m and a red PQD array composed of 23 × 13 micropores with a diameter of 45 $\mu$m are displayed in the inset of Figs. 4(e) and 4(f) under 365 nm UV light excitation. 91.5% of the green PQD pixels fall within the range of 74.6–76.5 and 90.2% of the red PQD pixels fall within the range of 72.6–74.5, as depicted in Figs. 4(e) and 4(f). In fact, according to the "Measure methods of light emitting diode (LED) displays" in the electronic industry standards of the People's Republic of China, the luminous uniformity ($I_{RJ}$) of the 28 × 18 green QD pixel array and 23 × 13 red QD pixel array can be calculated by

$$I_{RJ} = 1 - \frac{|I_i - \bar{I}|_{max}}{\bar{I}} \times 100\%, \quad (2)$$

where $I_i$ is the fluorescence intensity of the QD pixels, and $\bar{I}$ is the arithmetic average fluorescence intensity of 30 QD pixels selected randomly from all the QD pixels. The result indicates that the green and red QD pixels have a luminous uniformity of 98.837% and 97.754%, satisfying the national standard.

In conclusion, we have fabricated PQDCCLs based on laser drilling and micropore filling technology, with the characteristics of shorter process period, lower production cost, simpler operation process, and QDs saving compared to QDCCLs made using inkjet printing and photolithography. Due to their contactless feature with masks and chemical solvents, damage and waste of the PQDs are greatly reduced. However, it is worth noting that the micropore diameter was minimally restricted to 35 $\mu$m, owing to the limited light spot size of the fiber laser employed in this experiment. It will be possible to obtain an ultra-high resolution QDCCL with the aid of femtosecond laser interference lithography and micro-lens arrays. Additionally, both simulation analysis and experimental observation have proved that incorporating black SU8 photoresist as a light-blocking matrix effectively mitigates the issue of light crosstalk. By reusing laser drilling and micropore filling, we also achieved the manufacturing of a dual-color QDCCL with high luminance uniformity. These results show that QDCCLs fabricated by laser drilling and micropore filling provide a potential pathway for the commercialization of high-performance color-converted full-color displays by integrating with blue micro-LED.

See the supplementary material for the supporting content.

This work was financially supported by the National Key Research and Development Program (No. 2022YFB3604702) and the Jilin Scientific and Technological Development Program (No. 20200401056GX); the authors would like to appreciate Professor Haizheng Zhong and Dr. Fei Li from Hefei Innovation Research Institute of Beihang University for their valuable assistance in providing perovskite quantum dot UV curing gel.

## AUTHOR DECLARATIONS

### Conflict of Interest

The authors have no conflicts to disclose.

## Author Contributions

**Jiwei Li:** Conceptualization (equal); Investigation (equal); Writing – original draft (equal); Writing – review & editing (equal). **Baixuan Zhao:** Investigation (equal). **Yingze Zhao:** Investigation (equal). **Yupeng Chen:** Investigation (equal). **Jingqiu Liang:** Funding acquisition (equal); Supervision (equal); Writing – review & editing (equal). **Weibiao Wang:** Conceptualization (equal); Funding acquisition (equal); Supervision (equal); Writing – review & editing (equal). **Kaifeng Zheng:** Investigation (equal). **Wenchao Sun:** Investigation (equal). **Licai Zhu:** Investigation (equal). **Jin Tao:** Methodology (equal). **Panyuan Li:** Investigation (equal). **Kaili Fan:** Investigation (equal). **Jinguang Lv:** Investigation (equal). **Yuxin Qin:** Investigation (equal).

## DATA AVAILABILITY

The data that support the findings of this study are available within the article and its supplementary material.

## REFERENCES


[1] Y. Huang, E. L. Hsiang, M. Y. Deng, and S. T. Wu, Light: Sci. Appl. **9**, 105 (2020).
[2] X. Zhou, P. Tian, C. W. Sher, J. Wu, H. Liu, R. Liu, and H. C. Kuo, Prog. Quant. Electron. **71**, 100263 (2020).
[3] Y. Wu, J. Ma, P. Su, L. Zhang, and B. Xia, Nanomaterials **10**(12), 2482 (2020).
[4] A. R. Anwar, M. T. Sajjad, M. A. Johar, C. A. Hernández-Gutiérrez, M. Usman, and S. P. Łepkowski, Laser Photonics Rev. **16**(6), 2100427 (2022).
[5] K. Ding, V. Avrutin, N. Izyumskaya, Ü. Özgür, and H. Morkoç, Appl. Sci. **9**(6), 1206 (2019).
[6] S. Coe, W. K. Woo, M. Bawendi, and V. Bulović, Nature **420**(6917), 800–803 (2002).
[7] J. Lim, S. Jun, E. Jang, H. Baik, H. Kim, and J. Cho, Adv. Mater. **19**(15), 1927–1932 (2007).
[8] H. Ji, S. Cheng, P. Li, Y. Zhang, Z. Ge, and H. Zhong, Chin. Opt. **15**(1), 132 (2022).
[9] Y. Liu, F. Li, L. Qiu, K. Yang, Q. Li, X. Zheng, H. Hu, T. Guo, C. Wu, and T. W. Kim, ACS Nano **13**(2), 2042–2049 (2019).
[10] C. Jiang, L. Mu, J. Zou, Z. He, Z. Zhong, L. Wang, M. Xu, J. Wang, J. Peng, and Y. Cao, Sci. China Chem. **60**, 1349–1355 (2017).
[11] S. Shi, W. Bai, T. Xuan, T. Zhou, G. Dong, and R. J. Xie, Small Methods **5**(3), 2000889 (2021).
[12] H. V. Han, H. Y. Lin, C. C. Lin, W. C. Chong, J. R. Li, K. J. Chen, P. Yu, T. M. Chen, H. M. Chen, K. M. Lau, and H. C. Kuo, Opt. Express **23**(25), 32504 (2015).
[13] Z. Hu, Y. Yin, M. U. Ali, W. Peng, S. Zhang, D. Li, T. Zou, Y. Li, S. Jiao, S. Chen, C. Lee, H. Meng, and H. Zhou, Nanoscale **12**(3), 2103 (2020).
[14] Y. Wang, I. Fedin, H. Zhang, and D. V. Talapin, Science **357**(6349), 385 (2017).
[15] J. Harwell, J. Burch, A. Fikouras, M. C. Gather, A. Di Falco, and I. D. Samuel, ACS Nano **13**(4), 3823 (2019).
[16] P. P. Zhang, G. L. Yang, G. G. Kang, J. B. Shi, and H. Z. Zhong, Chin. J. Appl. Chem. **38**(9), 1175 (2021).
[17] H. Li, Y. Duan, Z. Shao, G. Zhang, H. Li, Y. Huang, and Z. Yin, Adv. Mater. Technol. **5**(10), 2000401 (2020).
[18] H. Y. Lin, C. W. Sher, D. H. Hsieh, X. Y. Chen, H. M. P. Chen, T. M. Chen, K. M. Lau, C. H. Chen, C. C. Lin, and H. C. Kuo, Photonics Res. **5**(5), 411 (2017).
[19] L. Huang, W. Zhang, X. Wei, Y. Wu, and B. Huang, *Study on Morphology of Quantum Dots Films Prepared by Inkjet Printing* (Springer, Nature Singapore, Singapore, 2023), p. 153.
[20] X. Liu, J. Li, P. Zhang, W. Lu, G. Yang, H. Zhong, and Y. Zhao, Nano Res. **15**(8), 7681 (2022).
[21] Z. Liu, C. H. Lin, B. R. Hyun, C. W. Sher, Z. Lv, B. Luo, F. Jiang, T. Wu, C. H. Ho, H. C. Kuo, and J. H. He, Light: Sci. Appl. **9**(1), 83 (2020).
[22] S. Lee and C. Lee, Polym. Adv. Technol. **30**(3), 749 (2019).
[23] Y. H. Kim, S. Koh, H. Lee, S. M. Kang, D. C. Lee, and B. S. Bae, ACS Appl. Mater. Interfaces **12**(3), 3961 (2020).
[24] H. M. Kim, M. Ryu, J. H. Cha, H. S. Kim, T. Jeong, and J. Jang, J. Soc. Inf. Disp. **27**(6), 347 (2019).
[25] W. Mei, Z. Zhang, A. Zhang, D. Li, X. Zhang, H. Wang, Z. Chen, Y. Li, X. Li, and X. Xu, Nano Res. **13**, 2485 (2020).
[26] W. Sun, F. Li, J. Tao, P. Li, L. Zhu, J. Li, J. Lv, W. Wang, J. Liang, and H. Zhong, Nanoscale **14**(16), 5994 (2022).
[27] H. Wang, H. Lin, C. Wang, L. Zheng, and X. Hu, J. Eur. Ceram. Soc. **37**(4), 1157 (2017).
[28] H. J. Wang and T. Yang, J. Eur. Ceram. Soc. **41**(10), 4997 (2021).
[29] Z. Lin and M. Hong, Ultrafast Sci. **2021**, 9783514.
[30] M. H. Hong, C. H. Liu, F. Ma, Z. C. Chen, B. Luk'yanchuk, L. P. Shi, and T. C. Chong, Proc. SPIE **7202**(24), 3605 (2009).
[31] Y. Yin, Z. Hu, M. U. Ali, M. Duan, Y. Wu, M. Liu, W. Peng, J. Hou, D. Li, X. Zhang, and H. Meng, Light **3**(3), 445 (2022).